



Contents lists available at ScienceDirect



Catalysis Today

journal homepage: www.elsevier.com/locate/cattod

Aerobic oxidative esterification of primary alcohols over Pd-Au bimetallic catalysts supported on mesoporous silica nanoparticles

Chih-Hsiang Tsai^a, Mengze Xu^b, Pranaw Kunal^b, Brian G. Trewyn^{a,b,*}

^a Department of Chemistry, Iowa State University, Ames, IA 50011, United States

^b Department of Chemistry, Colorado School of Mines, Golden, CO 80401, United States

ARTICLE INFO

Article history:

Received 3 October 2016

Received in revised form

22 December 2016

Accepted 25 January 2017

Available online xxx

Keywords:

Mesoporous silica nanoparticles

Bimetallic catalysis

Oxidative esterification

Tandem catalysis

ABSTRACT

We have prepared a series of mesoporous silica nanoparticle (MSN) supported Pd-Au bimetallic catalysts using a newly developed sequential impregnation method. These catalysts were fully characterized by various techniques including nitrogen sorption, powder X-ray diffraction, inductively coupled plasma mass spectrometry (ICP-MS), transmission electron microscopy (TEM) and high angle annular dark-field scanning transmission electron microscopy (HADDF-STEM). By using this synthetic approach, we observed metal nanoparticles (NP) with diameters of 1–2 nm homogeneously supported on the MSN. The catalytic performance of these MSN supported metal NPs was tested by aerobic oxidative esterification in a tandem reaction where primary alcohols are oxidized to their corresponding aldehydes and to esters in a subsequent reaction. We determined that Pd NPs are very efficient in the first step of oxidation; however, stagnant in the subsequent oxidation. On the contrary, Au NPs show slow reactivity in converting alcohols to aldehydes, but extraordinarily efficient in the oxidation of aldehydes to esters. By fine tuning the metal ratio, the bimetallic catalyst exhibits better reactivity and selectivity toward a variety of primary alcohols than the corresponding monometallic catalysts. In addition, we also found that the bimetallic Pd-Au@MSN catalysts can be recycled three times without a significant loss in activity.

© 2017 Elsevier B.V. All rights reserved.

1. Introduction

Selective oxidation of alcohols to the corresponding carbonyl compounds is a primary topic of interest in organic synthesis [1–6]. The resulting aldehyde, ketone, ester and acid products are valuable intermediates to fine chemical, pharmaceutical and agro-chemical industries [5,7,8]. Typically, this type of reaction is carried out in high yield using stoichiometric amounts of strong reagents such as transition metal oxidants or halo-oxoacids [9]. However, with emerging environmental and economic concerns, increased effort has been focused on the development of new types of catalysts to enhance catalytic reactivity and reduce chemical waste. Using molecular oxygen as an oxidant, aerobic oxidation of alcohols catalyzed by transition-metal catalysts including organometallic complexes and metal nanoparticles has attracted the attention of researchers worldwide [10–13]. Among these catalysts, supported metal nanoparticle catalysts show very interesting features and promising catalytic activities [1,10,14–16]. Not only can these

heterogeneous catalysts be easily separated and recycled several times, but they also exhibit extremely high reactivity and selectivity even under mild reaction conditions. For example, Clark and coworkers have reported the synthesis of palladium nanoparticles supported on SBA-15 type materials that demonstrate very efficient and selective aerobic oxidation of various alcohols [14,17]. A quantitative yield can be reached even with a relatively-inert alkyl substrate under ambient conditions. In addition, Hutchings et al. developed a TiO₂ supported Au-Pd catalyst which shows extremely high catalytic activity in aerobic oxidation of alcohols to aldehydes [3]. Later they demonstrated that this bimetallic catalyst can also efficiently oxidize toluene under 10 bar of oxygen to yield benzyl benzoate [18]. More recently, Wang et al. reported a graphene supported Au-Pd catalyst which exhibits high catalytic activity in methanol selective oxidation to methyl formate [19]. Qiu et al. put forward an amphiphilic hollow mesoporous shell and an Au@Pd bimetal nanoparticle core which shows excellent catalytic activity and stability in aerobic oxidation of alcohols in water [20].

Functionalized mesoporous silica materials represent ideal inorganic supports for immobilizing catalysts due to their high surface area (>700 m² g⁻¹), defined pore structure, tunable pore diameter (2–10 nm) and narrow pore size distribution. It has been reported that the confined mesochannels can effectively control

* Corresponding author at: Department of Chemistry, Colorado School of Mines, Golden, CO, 80401, United States.

E-mail address: btrewyn@mines.edu (B.G. Trewyn).

the agglomeration of metal nanoparticles [15,21–28]. Furthermore, surface-bound ligands/functionalities can be used to stabilize the metal NPs, whose high surface energy frequently leads to the aggregation of nanoparticles [17,29–33]. Several studies involved in supporting metal nanoparticles on the mesoporous silica materials, such as Pd, Pt, Au, Rh, Ir and Ru on MCM/SBA-type materials, have revealed superior catalytic performances on many types of chemical transformations [15,16,34–38]. The synergistic effect has also been observed in some bimetallic systems [1,17,39]. For example, Chen and coworkers reported a Pd/Au bimetallic catalyst system exhibiting enhanced reactivity and selectivity toward the solvent-free aerobic oxidation of alcohols, where the Pd and Au complexes were coordinated onto the amine-functionalized SBA-16 silica support prior to their reduction to nanoparticles [33]. In another example, Yang et al. reported a high performance Pd/Au bimetallic catalytic system demonstrating hydrogenation of cinnamaldehyde [40].

Herein, we report the synthesis and catalytic properties for a tandem aerobic oxidative esterification reaction of a series of mono- and bimetallic Pd/Au catalysts supported on mesoporous silica nanoparticles (MSNs) through a sequential impregnation method (**Scheme 1**). This synthetic approach has shown to be effective in producing homogeneously distributed metal NPs on the MSN support and good control of the incorporated metal ratio. We compared the catalytic performance of our MSN catalysts with several commercially available Au and Pd catalysts, such as Au@TiO₂, Au@Al₂O₃ and Pd/C, in the aerobic oxidative esterification of benzyl alcohol with methanol. Several primary alcohols were also selected for oxidation to demonstrate the generality of this bimetallic catalyst. Interestingly, monometallic Pd@MSN catalyst exhibited high reaction conversion but poor selectivity, leading to benzaldehyde as the major product. On the contrary, catalysts containing monometallic Au showed superior selectivity to ester product but suffered from sluggish reactivity. Compared to their monometallic counterparts, the bimetallic Pd-Au@MSN catalyst was more efficient in both reactivity and selectivity. An in-depth study of different substrates was also performed with the most efficient Pd-Au bimetallic MSN catalyst. Finally, we tested the recyclability of the bimetallic Pd-Au@MSN catalyst in the same reaction conditions.

2. Materials and methods

2.1. Reagents and materials

All chemicals were used as received without further purification. Tetraethoxysilane (TEOS) was purchased from Gelest, Inc. Au@TiO₂ (1 wt% Au) and Au@Al₂O₃ (1 wt% Au) were purchased from Strem Chemicals, Inc. Other chemical reagents were purchased from Sigma-Aldrich, Inc.

2.2. Synthesis of mesoporous silica nanoparticle (MSN)

The MSN material was synthesized via a previously reported co-condensation method [41,42]. Typically, a mixture of cetyltrimethylammonium bromide (CTAB, 2.0 g, 5.5 mmol) and 2.0 M of NaOH_(aq) (7.0 ml, 14 mmol) in 480 ml of deionized water was heated at 80 °C for 30 min. To this solution, tetraethoxysilane (TEOS, 10.0 ml, 44.8 mmol) was injected rapidly. A milky solution formed within 2 min post injection. The resulting reaction mixtures were stirred at 80 °C for 2 h. The solid product was then filtered, washed with copious amounts of deionized water and methanol and dried overnight under high vacuum. A hydrothermal treatment of the as-made MSN material was performed by soaking MSN material (3.0 g) in 20 ml of DI water. The reaction mixture was incubated at 100 °C for 6 h. The solid product was filtered

and dried under high vacuum for 24 h. To remove the surfactant molecules, a solution of MSN materials (2.0 g) and 2.0 ml of concentrated HCl in 200 ml of methanol was stirred at 60 °C for 6 h. The resulting surfactant-free MSNs were filtered, washed with water and methanol, and dried under vacuum for 24 h.

2.3. Synthesis of bis(ethylenediamine) gold (III) chloride – Au(en)₂Cl₃

The synthetic procedure of this Au complex precursor has been reported in the literature [31]. Typically, ethylenediamine (0.45 ml, 6.7 mmol) was slowly added into 10 ml of aqueous solution of HAuCl₄·3H₂O (1.0 g, 2.54 mmol) until the solution turned transparent. This solution was stirred for 30 min at room temperature. Anhydrous ethanol (70 ml) was then added into the solution and a precipitate formed immediately. The solid product was filtered, followed by washing with ethanol and drying overnight under high vacuum.

2.4. Synthesis of monometallic Pd@MSN

Surfactant-free MSN materials (500 mg) was pre-dried under vacuum at 90 °C for 6 h to remove physisorbed water. To this reaction, a solution of Pd(OAc)₂ (28 mg, 0.125 mmol) in 15 ml dry toluene was injected. The reaction was stirred at 35 °C for 3 h, followed by filtration and wash with 300 ml of toluene and 100 ml of methanol, and dried under vacuum for 24 h to obtain a brownish solid product denoted as Pd-complex-MSN. The Pd-complex-MSN materials were then reduced by flowing H₂ at a rate of 30 ml min⁻¹ at 250 °C for 3 h to yield a gray colored final product (Pd@MSN).

2.5. Synthesis of monometallic Au@MSN

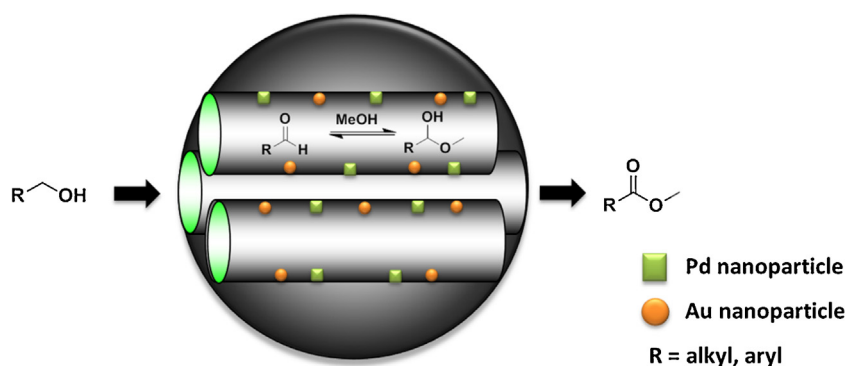
Typically, Au(en)₂Cl₃ (36 mg, 0.085 mmol) was dissolved in 60 ml of DI water. The pH value of this solution was adjusted by adding 1.0 M NaOH solution to reach a pH of 10.0. Subsequently, 500 mg of surfactant-free MSN materials were added. The pH value of this solution dropped to around 6 immediately due to the intrinsic acidity of the high surface area silica material. By adding 1.0 M NaOH solution, the final pH value of the reaction mixture was tuned to 9.5. The mixture was stirred for an additional 2 h at room temperature, followed by filtration and wash with 300 ml of water and 100 ml of methanol, and dried under vacuum for 24 h to obtain a yellow colored solid product denoted as Au-complex-MSN. The reduction of the Au-complex-MSNs was carried out by flowing H₂ at a rate of 30 ml min⁻¹ at 250 °C for 3 h to yield a purple colored final product (Au@MSN).

2.6. Synthesis of bimetallic Pd-Au@MSNs

A sequential impregnation method was applied to synthesize the bimetallic MSN materials. The pre-synthesized Au-complex-MSN (500 mg) was dried at 90 °C for 6 h to remove physisorbed water molecules. A solution of Pd(OAc)₂ (17.7 mg, 0.079 mmol) in dry toluene (25 ml) was then added. The solution was stirred at 35 °C for 3 h, followed by filtration and washing with copious amounts of toluene and methanol, and dried under vacuum for 24 h. The reduction procedure was the same as previously described. By tuning the molar ratio of Pd and Au, three bimetallic Pd-Au@MSNs-x (where x indicates Pd/Au molar ratio) catalysts were synthesized.

2.7. Aerobic oxidative esterification of benzyl alcohol for comparison of catalysts

A mixture of benzyl alcohol (108 mg, 1 mmol), K₂CO₃ (138 mg, 1 mmol), and catalysts (0.005 mmol, 0.5 mol% on the total metal



Scheme 1. Schematic representation of Pd-Au bimetallic MSN catalyzed aerobic oxidative esterification of alcohols in methanol.

basis) in dry methanol (2 ml) was prepared in a reaction tube at room temperature. The reactor was then purged and filled with pure oxygen (filled balloon). The resulting mixture was then stirred at 60 °C under an oxygen atmosphere (balloon) for 1 h. After completion of the reaction, the solid catalyst was filtered off and washed with methanol (2 ml × 3). The filtrate was combined and analyzed by GC (Hewlett-Packard 5890 GC equipped with HP-5 column) using anisole as the internal standard.

2.8. Aerobic oxidative esterification of alcohols catalyzed by Pd-Au@MSN-1.8

The reaction procedure is the same as previously described but with varied reaction time. The results were analyzed by GC (Hewlett-Packard 5890 GC equipped with HP-5 column) and an Agilent Technologies 7890A gas chromatograph equipped with a HP-5 column in-line with a 5975C mass detector.

2.9. Test of recyclability of Pd-Au@MSN-1.8 and Pd@MSN

A mixture of benzyl alcohol (324 mg, 3 mmol), K_2CO_3 (414 mg, 3 mmol), and Pd-Au@MSN-1.8 catalyst (66 mg, 0.5 mol% on the total metal basis) in dry methanol (6 ml) was prepared in a reaction vessel at room temperature. The reaction mixture was purged and filled with pure oxygen (filled balloon). The resulting mixture was stirred at 60 °C under an oxygen atmosphere (balloon) for 1 h. After completion of reaction, the solid catalyst was filtered off and washed with methanol (2 ml × 3). The filtrate was combined and analyzed by GC using anisole as the internal standard. The catalyst was then recovered by washing with water (10 ml × 3) and methanol (10 ml × 3), and dried under vacuum for 24 h. The recovered catalyst was then used for subsequent runs. The recyclability of Pd@MSN was measured by following the same procedures as described above, using a 0.5 mol% metal ratio of benzyl alcohol.

2.10. Characterization methods

Surface analysis of these MSN catalysts was performed by nitrogen sorption isotherms at 77 K with a Micromeritics ASAP 2020 surface area and porosity analyzer. The surface area and median pore diameter were evaluated by the Brunauer-Emmett-Teller (BET) and Barrett-Joyner-Halenda (BJH) methods, respectively. The powder diffraction patterns of these catalysts were measured by a Rigaku Ultima IV X-Ray Diffractometer using a $\text{Cu K}\alpha$ radiation source. Low angle diffraction with a 2θ range of 1.5–10° was used to investigate the long-range order of the materials. High angle diffraction with a 2θ range from 10 to 90° was used to determine the degree of crystallinity of metals inside the mesopores of MSN catalysts. Tecnai G² F20 transmission electron microscopy (TEM) operated at 200 kV was used to examine the mesostructure of mate-

rials. The metal content of these MSN catalysts was quantified by Hewlett-Packard 4500 ICP-OES after acid digestion of the materials.

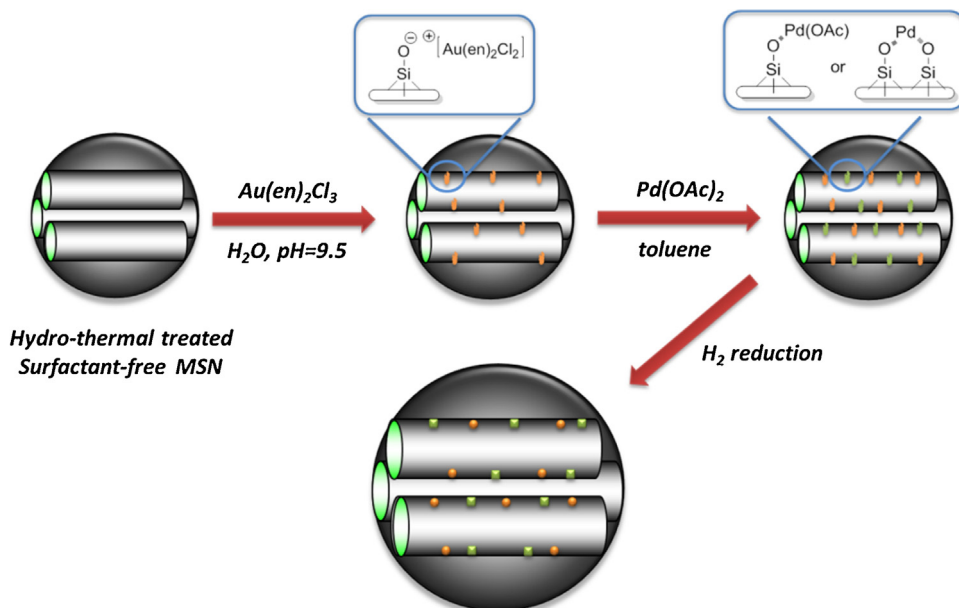
3. Results and discussion

3.1. Material synthesis

As illustrated in **Scheme 2**, the Pd-Au bimetallic MSN catalysts (Pd-Au@MSNs) were synthesized via a sequential impregnation method. Gold was introduced into the MSN support in an aqueous solution through a deposition-precipitation method developed by Dai et al., where $\text{Au}(\text{en})\text{Cl}_3$ was used as the precursor [31]. By fine tuning the pH of the MSN suspension, positively charged Au complexes can be well-distributed over the negatively charged silica surface due to strong electrostatic interactions. Subsequently, $\text{Pd}(\text{OAc})_2$ was impregnated into the gold-containing MSN (Au-complex-MSN) in toluene, followed by moderate hydrogen reduction to form metal nanoparticles on the surface of MSN support. With this method, metal precursors are efficiently loaded onto the MSN surface without the assistance of chelating ligands, such as amine groups, resulting in a homogeneous distribution of metal nanoparticles. Several studies have disclosed that using strong ligands to bind the metal complexes could efficiently control the distribution and the size of metal nanoparticles [17,22–26,29]. However, it has also been reported that the ligand-assisted strategy would sometimes lead to inferior catalytic performance due to strong interactions between chelating ligands and the metal surface [29]. In addition, it is also plausible that some organic ligands would participate in the reaction resulting in complicated systems, e.g. amine groups may be oxidized to imine or enamine under metal nanoparticles catalyzed oxidation reaction [43]. In general, the silanol groups on the silica surface are not strong ligands for coordinating Pd metal. Thus, the efficiency of Pd impregnation on pure silica surface was usually low [43–45]. However, after base-treatment the deprotonated silanol groups would become electron-rich and be able to effectively coordinate with the electron-deficient Pd metal center. As a result, we found that the molar ratio of Pd and Au elements can be easily controlled by using our synthetic method due to the fact that the measured loading of metals is very close to the amount of metal precursors we initially introduced. Monometallic Pd- and Au@MSN catalysts were also synthesized via the same procedure for comparison of catalytic reactivity.

3.2. Characterization of MSN catalysts

These mono- and bi-metallic MSN catalysts were fully characterized by various techniques. As shown in **Fig. 1**, the high angle annular dark-field scanning transmission electron microscopy (HADDF-STEM) images clearly show that Pd and Au nanoclusters



Scheme 2. Schematic representation of the synthesis of bimetallic Pd-Au@MSN catalyst.

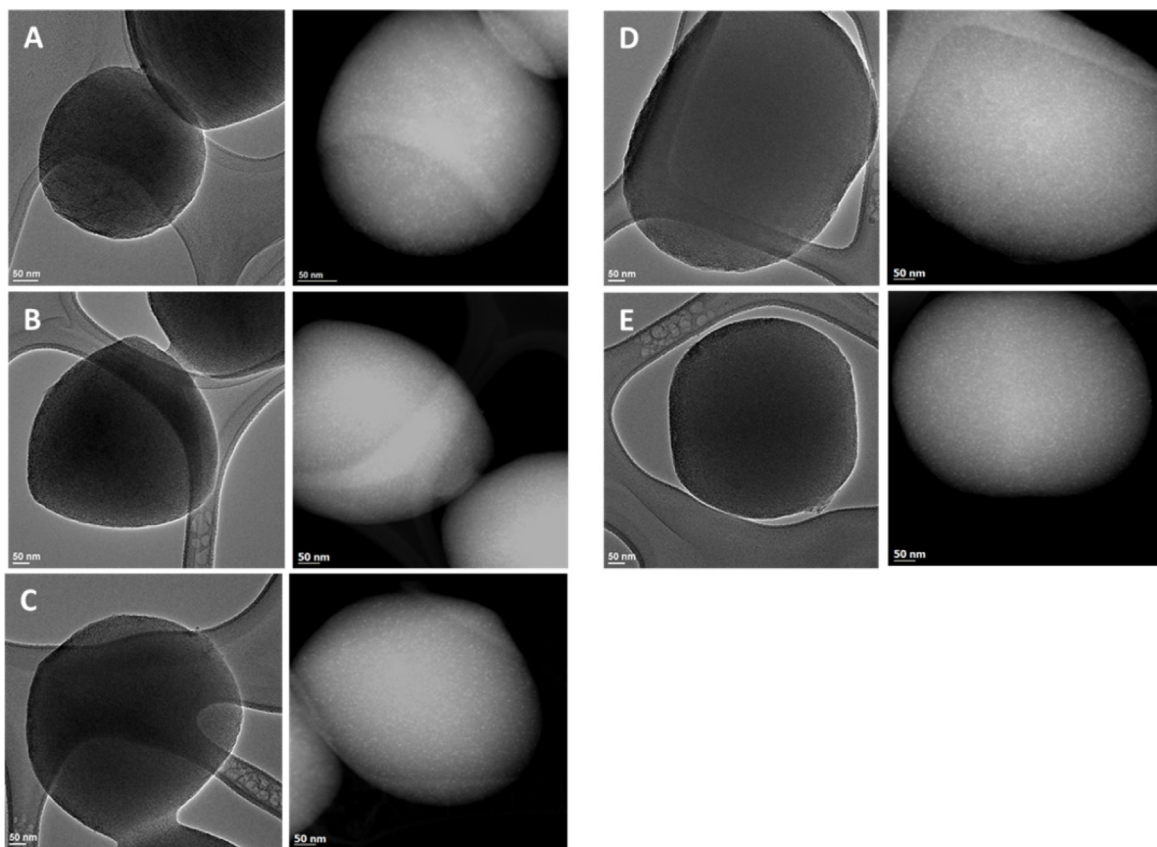


Fig. 1. TEM images of bimetallic MSN catalysts. Bright field (left) and dark field (right). A). Pd@MSN; B). Au@MSN; C). Pd-Au@MSN-1.8; D). Pd-Au@MSN-1.0; E). Pd-Au@MSN-0.55.

are well-distributed on the surfaces of the MSN catalysts. The diameter of metal particles was estimated around 2 nm by visual analysis of these images. In addition, there are no apparent aggregates of metals observed in any of these samples. Energy-dispersive X-ray spectroscopy (EDX) was also applied to determine the elemental composition of Pd-Au@MSN catalyst, as shown in Fig. S1. Both metal

elements are clearly detected in the case of bimetallic Pd-Au@MSN catalysts; however, it is still difficult to confirm if a Pd-Au alloy, core shell or well-separated metal clusters were formed inside the Pd-Au@MSN catalyst due to the limits on resolution. Figs. 2 and 3 show the powder X-ray diffraction patterns of these MSN catalysts. As illustrated in Fig. 2, at low angle range ($2\theta = 1.5\text{--}10^\circ$) three dis-

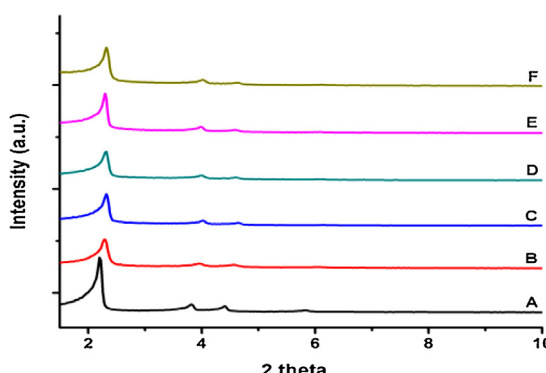


Fig. 2. Low angle powder X-ray diffraction of MSN catalysts. A). MSN; B). Pd@MSN; C). Au@MSN; D). Pd-Au@MSN-1.8; E). Pd-Au@MSN-1; F). Pd-Au@MSN-0.55.

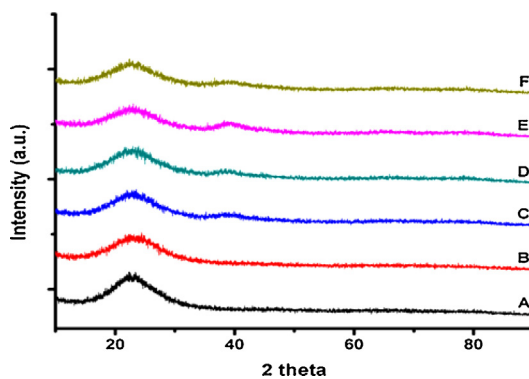


Fig. 3. High angle powder X-ray diffraction of MSN catalysts. A). MSN; B). Pd@MSN; C). Au@MSN; D). Pd-Au@MSN-1.8; E). Pd-Au@MSN-1; F). Pd-Au@MSN-0.55.

tinct peaks are observed that correspond to 2D-hexagonal patterns in all samples, indicating that the mesoporous structure of these MSN catalysts remained intact after the impregnation and reduction processes. On the other hand, at high angle range there is only one small peak at around $2\theta = 40^\circ$ which is diffracted from Au[111] and/or Pd[111] phase along with the characteristic broad peak of pure amorphous silica at around $2\theta = 22^\circ$ (Fig. 3) [46,47]. This result implies that the sizes of the metal clusters are relatively small and no large crystalline domain exist, which is in full agreement with TEM images.

Complemented to XRD results, nitrogen sorption isotherm analyses provided the bulk-average information of the mesoporous materials. As shown in Fig. S2, the plots obtained are typical type IV isotherms without hysteresis loops for all MSN catalysts. In addition, as summarized in Table 1 the synthesized catalysts exhibited an approximate BET surface area of $900 \text{ m}^2 \text{ g}^{-1}$, and a narrow size distribution at around 2.7 nm (Fig. S3), which are slightly reduced when compared to MSN (Table 1, Entry 1).

These results also suggest that the formed Pd and Au nanoparticles do not block the mesoporous channel of MSN catalysts, assuring the accessibility of the catalytic metal nanoparticles inside the mesopores. The actual loading of metal content of these MSN catalysts was determined by ICP-OES analysis and the results were summarized in Table 1. The measured loading is very close to the amount introduced, indicating this sequential impregnation method is very efficient and easy to control the molar ratio of bimetals.

3.3. Catalytic results

To compare catalytic performance of the mono- and bi-metallic MSN catalysts with commercially available solid supported gold

and palladium catalysts, the aerobic oxidative esterification of benzyl alcohol was carried out in methanol at 60°C with 0.5 mol% catalyst and one equivalent amount of K_2CO_3 . As shown in Table 2, the bimetallic Pd-Au@MSN-1.8 catalyst exhibits the highest catalytic reactivity among all catalysts tested here, which results in a full conversion of benzyl alcohol to yield the ester product quantitatively in 1 h. It is interesting to note that all Pd-containing catalysts (Table 2, Entry 1–2, 4–6) show higher benzyl alcohol conversion than monometallic Au catalysts (Table 2, Entry 3, 7–8). However, monometallic Pd catalysts (Entry 1–2) suffer from poor selectivity with a yield of only 50% methyl benzoate. On the contrary, reactions catalyzed by Au-containing catalysts exhibit better selectivity to the ester product. The major byproduct is benzaldehyde, which is the intermediate of this tandem oxidative reaction. These results directly suggest that Pd catalysts can effectively catalyze the oxidation of benzyl alcohol to form benzaldehyde but they are retarded in converting benzaldehyde to methyl benzoate. Compared to palladium, supported Au catalysts are very selective toward this reaction. The high selectivity of Au catalyst can be attributed to its high catalytic efficiency on the oxidative esterification of aldehyde, while the *in situ* generated benzaldehyde would be rapidly converted to methyl benzoate [48–50]. The rate determining step (RDS) of gold catalyzed aerobic oxidation reaction of alcohol has been reported to be the dehydrogenation of the alcohol to form its corresponding aldehyde [48]. Therefore, the slow RDS at the first step of the oxidation reaction limits the overall catalytic performance of monometallic supported Au catalysts. Comparing the catalytic performance of three bimetallic MSN catalysts, we can clearly observe a trend that catalysts with higher Pd to Au ratio lead to higher reactivity. In addition, the bimetallic Pd-Au@MSN-1.8 catalyst appears to be more efficient than monometallic Pd catalysts in terms of benzyl alcohol conversion, suggesting a synergistic effect which supports previous reports [1,17,39,51–53].

It is also interesting to note that Au@MSN shows comparable reactivity with Au@ Al_2O_3 and Au@ TiO_2 since SiO_2 has been reported to be poorer support than Al_2O_3 and TiO_2 in the case of oxidation of benzyl alcohol [54–57]. This may be attributed to the large surface area of MSN, around 4 and 10 times higher than Al_2O_3 and TiO_2 , respectively; providing better diffusion of substrates and accessibility to the catalyst. Based on the above mentioned results, we have demonstrated the bimetallic Pd-Au@MSN catalytic system can significantly enhance the reactivity of the aerobic oxidative esterification of benzyl alcohol. Further interests on metal–metal interaction, metal–support interaction and metal size effect in determining the catalytic performance are still under investigation.

Several examples of aerobic oxidative esterification catalyzed by Pd-Au@MSN-1.8 are summarized in Table 3. Most aromatic alcohols containing both electron-donating and electron-withdrawing groups in the *para*-position were converted to the corresponding methyl esters in high yields (entry 1–3, 5 and 7). Heteroaromatic 2-pyridyl methanol and cinnamyl alcohol (entry 6 and 11) were also oxidized to the corresponding methyl ester in decent yields. On the contrary, the oxidation of aliphatic alcohols needed extended reaction time to achieve moderate yields (entry 8–9). The poor reactivity of aliphatic alcohols could be due to slow oxidation of the first step of the reaction since we did not observe the formation of the intermediate aldehyde after the reaction. It is noteworthy that *p*-chlorobenzyl alcohol was not oxidized to its corresponding ester or aldehyde (entry 4). Instead, the major product was methyl benzoate (63% yield). This result implies that an oxidative insertion reaction followed by a reductive elimination occurred along with the aerobic oxidative esterification reaction of the alcohol. It has been well documented that Pd nanoparticle catalysts can efficiently catalyze Suzuki coupling reactions [58–60]. However, this phenomenon is not usually seen in most aerobic oxidation reaction conditions.

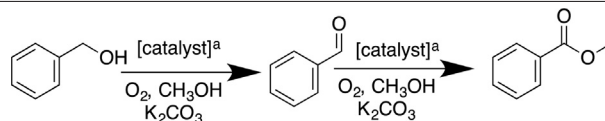
Table 1

Summary of physical properties of supported catalysts.

Entry	Catalyst	Pd (wt%) ^a	Au (wt%) ^a	Mole ratio	S_{BET} ($m^2 g^{-1}$) ^b	W_{BJH} (nm) ^b	Pore volume ($cm^3 g^{-1}$) ^b
1	MSN	–	–	–	1038	3.1	1.01
2	Pd@MSN	1.32	NA	–	938	2.8	0.79
3	Au@MSN	NA	1.63	–	878	2.7	0.76
4	Pd-Au@MSN (1.8:1)	1.57	1.59	1.82	865	2.7	1.77
5	Pd-Au@MSN (1:1)	1.15	2.17	0.97	873	2.7	0.81
6	Pd-Au@MSN (1:1.8)	0.84	2.89	0.54	883	2.7	0.80
7	Au@TiO ₂ ^c	NA	1	–	40–50	NA	–
8	Au@Al ₂ O ₃ ^c	NA	1	–	200–260	NA	–
9	Pd on activated charcoal ^c	5	NA	–	868	NA	0.54

^a The metal content was determined by ICP-OES analysis.^b Specific surface area (S_{BET}) and mean pore diameter (W_{BJH}) were obtained from nitrogen sorption analysis. The specific surface area was calculated by BET method and the mean pore diameter was calculated by BJH method.^c Information acquired from manufacturers' websites.**Table 2**

Comparison of catalytic performance of catalysts on aerobic oxidative esterification of benzyl alcohol.

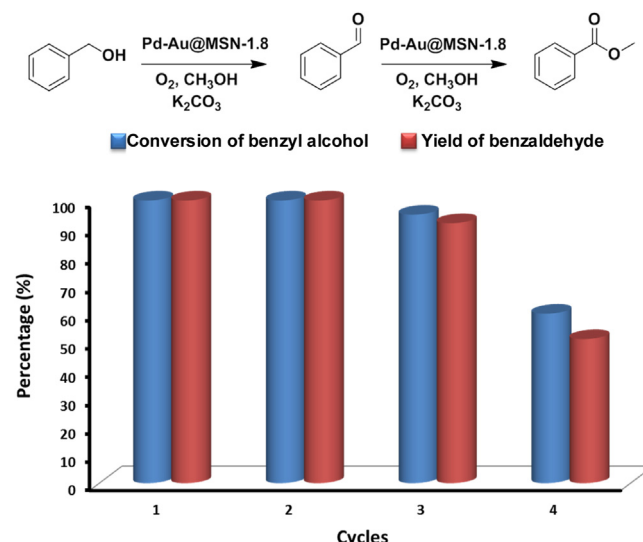


Entry	Catalyst	Conversion (%) ^b	Yield (% ester) ^c	Selectivity ^d
1	Pd/C	88	49	55.7
2	Pd@MSN	89	43	48.3
3	Au@MSN	38	37	97.3
4	Pd-Au@MSN-1.8	>99	>99	>99
5	Pd-Au@MSN-1	85	83	97.6
6	Pd-Au@MSN-0.55	61	60	98.4
7	Au@TiO ₂	31	30	96.7
8	Au@Al ₂ O ₃	39	39	>99

^a Reaction condition is detailed in the experimental section. Reactivity results were determined by GC using anisole as the internal standard.^b Percent conversion of benzyl alcohol.^c Percent yield of benzyl benzoate.^d Yield/conversion x 100%.

Therefore, this result suggests that our Pd-Au@MSN catalyst may have potential in catalyzing oxidative coupling reactions. In most cases, the major byproducts are the corresponding aldehydes. However, in the case of methyl 4-(hydroxymethyl)benzoate (Entry 7) the only byproduct observed was methyl 4-methylbenzoate instead of the aldehyde intermediate, which may result from a dehydroxylation reaction. This observation supports the reaction mechanism proposed by Hutchings et al., in which hydrides were generated *in situ* on the metal surface even under reaction condition with oxygen atmosphere [61].

The fidelity of heterogeneous catalysis in the case of Pd NPs catalyzed reaction is still in debate. It has been suggested that palladium nanoparticles would serve as reservoirs which release the Pd atoms to the solution and catalyze the reaction homogeneously [62]. In addition, catalyst leaching has always been a concern of supported metal catalysts. To rule out the contribution of homogeneous catalysis, the reaction with benzyl alcohol was conducted in the presence of Pd-Au@MSN-1.8 for 30 min to obtain a conversion of 78% and a yield of 63%. The solid catalyst was then hot-filtered and the reaction solution was transferred to another reaction vessel containing K₂CO₃. The catalyst-free solution was then stirred at 60 °C under O₂ atmosphere for additional 24 h, but no further reaction took place. In addition, the reaction solution was subsequently analyzed by ICP-OES and no metal (Pd and Au) species were detected within the detection limit. Hence, these results suggested that the supported Pd and Au nanoparticles were indeed securely confined inside the mesopores of MSN material and would not leach to the solution during the course of the reaction.

**Fig. 4.** Recyclability test of Pd-Au@MSN-1.8. Reactions were carried out under 60 °C for 1 h with 0.5 mol% Pd-Au@MSN-1.8.

To test the recyclability of this bimetallic MSN catalyst, an aerobic oxidative esterification with benzyl alcohol was performed in the presence of Pd-Au@MSN-1.8 catalyst. Fig. 4 shows the recyclability of the MSN catalyst for four cycles. Both conversion and yield were maintained as >99% in the first two cycles. They started dropping during the third run and declined significantly for the next

Table 3Catalytic performance of Pd-Au@MSN-1.8 on the oxidation of various alcohols.^a

Entry	Substrate	Conversion (%) ^b	Yield (% ester) ^c	Selectivity ^d
1		>99	>99	100
2		>99	>99	100
3		>99	>99	100
4 ^e		81	11	13.5
5		93	65	70
6		>99	76	76
7 ^f		>99	86	86
8 ^g		72	72	100
9 ^g	CH ₃ (CH ₂) ₁₁ OH	56	56	100
10 ^h		98	92	93.8
11 ^h		>99	>99	100

^a Reactions were carried out at 60 °C for 4 h with 0.5 mol% Pd-Au@MSN-1.8 and 0.5 M substrate concentration in methanol. Reactivity results were determined by GC-MS using anisole as an internal standard.

^b Percent conversion of benzyl alcohol.

^c Percent yield of benzyl benzoate.

^d Yield/conversion x 100%.

^e Methyl benzoate is the major product.

^f Methyl 4-methylbenzoate is the major byproduct.

^g 20 h reaction time.

^h Reactivity determined by NMR with *p*-xylene as internal standard.

cycle. As a comparison, in the recyclability test of Pd@MSN shown in Fig. S5, the conversion and yield decreased dramatically immediately following the first run. To investigate the catalyst deactivation, Pd-Au@MSN-1.8 catalyst was examined by TEM after the third cycle. As shown in Fig. S3, the mesostructure of MSN is less defined and its original 2d-hexagonal mesopores has been converted to a wormlike structure. This deformation of MSN support would likely reduce the accessibility of catalytic sites inside the MSN, causing the decline in reactivity. Another STEM mode image, also shown in Fig. S3, shows that the metal nanoparticles are mostly confined within the mesopores after three runs of reactions even though some small agglomerates are sporadically observed. It is also evident that mesoporous silica is a good solid support, preventing the supported metal clusters from agglomeration due to its confined mesoporosity.

Future investigations in this area will involve measuring the effects that pore size has on the diffusion of reactants into and products out of the mesopores. Another focus will be to modify the pore surface with organic functional groups to control the molecular dif-

fusion as was shown for MSN tethered molecular catalyst systems [41].

4. Conclusions

A series of MSN supported Pd-Au bimetallic NPs as catalysts for aerobic oxidative esterification has been synthesized through a sequential impregnation method. We have shown that samples prepared by this approach exhibit homogeneously distributed metal nanoparticles within the mesopores. The Pd-Au bimetallic catalyst reveals superior catalytic reactivity and selectivity over all monometallic catalysts including commercial available Pd/C, Au@TiO₂ and Au@Al₂O₃. The reaction kinetics and mechanism were also discussed. In addition, a great scope of primary alcohols has been tested, and showed quantitative yields in most cases, indicating a general application of our Pd-Au@MSN catalyst. For recyclability, we have found that these MSN catalysts can be reused three times without losing activity.

Acknowledgement

This research was supported by the U.S. Department of Energy, under Award Number DE-SC0001298 (as part of the Center for Catalytic Hydrocarbon Functionalization, an Energy Frontier Research Center).

Appendix A. Supplementary data

Supplementary data associated with this article can be found, in the online version, at <http://dx.doi.org/10.1016/j.cattod.2017.01.046>.

References

- [1] A. Abad, P. Concepcion, A. Corma, H. Garcia, *Angew. Chem. Int. Ed.* **44** (2005) 4066–4069.
- [2] J.K. Edwards, B.E. Solsona, P. Landon, A.F. Carley, A. Herzing, C.J. Kiely, G.J. Hutchings, *J. Catal.* **236** (2005) 69–79.
- [3] D.I. Enache, J.K. Edwards, P. Landon, B. Solsona-Espriu, A.F. Carley, A.A. Herzing, M. Watanabe, C.J. Kiely, D.W. Knight, G.J. Hutchings, *Science* (Washington, DC, U.S.) **311** (2006) 362–365.
- [4] R.A. Sheldon, I.W.C.E. Arends, G.-J. ten Brink, A. Dijksman, *Acc. Chem. Res.* **35** (2002) 774–781.
- [5] R.A. Sheldon, J.K. Kochi, *Metal-Catalyzed Oxidation of Organic Compounds*, Academic Press, New York, 1981.
- [6] G.-J. ten Brink, I.W.C.E. Arends, R.A. Sheldon, *Science* (Washington, D. C.) **287** (2000) 1636–1639.
- [7] M. Hudlicky, *Oxidations in Organic Chemistry*, American Chemical Society, Washington, DC, 1990.
- [8] U.R. Pillai, E. Sahle-Demessie, *Appl. Catal. A* **245** (2003) 103–109.
- [9] M.B. Smith, *March's Advanced Organic Chemistry*, 7th ed., Wiley-Interscience, New York, 2013.
- [10] T. Mallat, A. Baiker, *Chem. Rev.* (Washington, DC, U.S.) **104** (2004) 3037–3058.
- [11] T. Punniyamurthy, S. Velusamy, J. Iqbal, *Chem. Rev.* **105** (2005) 2329–2363.
- [12] M.J. Schultz, M.S. Sigman, *Tetrahedron* **62** (2006) 8227–8241.
- [13] H. Miyamura, R. Matsubara, Y. Miyazaki, S. Kobayashi, *Angew. Chem. Int. Ed.* **46** (2007) 4151–4154.
- [14] B. Karimi, A. Zamani, S. Abedi, J.H. Clark, *Green Chem.* **11** (2009) 109–119.
- [15] R.J. White, R. Luque, V.L. Budarin, J.H. Clark, D.J. MacQuarrie, *Chem. Soc. Rev.* **38** (2009) 481–494.
- [16] A. Corma, H. Garcia, *Chem. Soc. Rev.* **37** (2008) 2096–2126.
- [17] B. Karimi, S. Abedi, J.H. Clark, V. Budarin, *Angew. Chem. Int. Ed.* **45** (2006) 4776–4779.
- [18] L. Kesavan, R. Tiruvalam, M.H. Ab Rahim, M.I. bin Saiman, D.I. Enache, R.L. Jenkins, N. Dimitratos, J.A. Lopez-Sanchez, S.H. Taylor, D.W. Knight, C.J. Kiely, G.J. Hutchings, *Science* (Washington, DC, U.S.) **331** (2011) 195–199.
- [19] R.Y. Wang, Z.W. Wu, C.M. Chen, Z.F. Qin, H.Q. Zhu, G.F. Wang, H. Wang, C.M. Wu, W.W. Dong, W.B. Fan, J.G. Wang, *Chem. Commun. (Cambridge, U.K.)* **49** (2013) 8250–8252.
- [20] H.B. Zou, R.W. Wang, J.Y. Dai, Y. Wang, X. Wang, Z.T. Zhang, S.L. Qiu, *Chem. Commun. (Cambridge, U.K.)* **51** (2015) 14601–14604.
- [21] Y. Doi, A. Takai, Y. Sakamoto, O. Terasaki, Y. Yamauchi, K. Kuroda, *Chem. Commun. (Cambridge, U.K.)* **46** (2010) 6365–6367.
- [22] X.C. Liu, D.S. Chen, L. Chen, R.X. Jin, S.X. Xing, H.Z. Xing, Y. Xing, Z.M. Su, *Chem. Eur. J.* **22** (2016) 9293–9298.
- [23] H.J. Wang, H.Y. Jeong, M. Imura, L. Wang, L. Radhakrishnan, N. Fujita, T. Castle, O. Terasaki, Y. Yamauchi, *J. Am. Chem. Soc.* **133** (2011) 14526–14529.
- [24] B. Lee, Z. Ma, Z. Zhang, C. Park, S. Dai, *Microporous Mesoporous Mat.* **122** (2009) 160–167.
- [25] M. Perez-Cabero, J. El Haskouri, B. Solsona, I. Vazquez, A. Dejoz, T. Garcia, J. Alvarez-Rodriguez, A. Beltran, D. Beltran, P. Amoros, *J. Mater. Chem.* **20** (2010) 6780–6788.
- [26] J. Sun, X. Bao, *Chem. Eur. J.* **14** (2008) 7478–7488.
- [27] K.C.W. Wu, Y. Yamauchi, *J. Mater. Chem.* **22** (2012) 1251–1256.
- [28] V. Malgras, Q.M. Ji, Y. Kamachi, T. Mori, F.K. Shieh, K.C.W. Wu, K. Ariga, Y. Yamauchi, *Bull. Chem. Soc. Japan* **88** (2015) 1171–1200.
- [29] Y.-S. Chi, H.-P. Lin, C.-Y. Mou, *Appl. Catal. A* **284** (2005) 199–206.
- [30] C.-M. Yang, B. Zibrowius, F. Schueth, *Chem. Commun. (Cambridge, U.K.)* (2003) 1772–1773.
- [31] H. Zhu, C. Liang, W. Yan, S.H. Overbury, S. Dai, *J. Phys. Chem. B* **110** (2006) 10842–10848.
- [32] C.-M. Yang, H.-A. Lin, B. Zibrowius, B. Spliethoff, F. Schueth, S.-C. Liou, M.-W. Chu, C.-H. Chen, *Chem. Mater.* **19** (2007) 3205–3211.
- [33] Y. Chen, H. Lim, Q. Tang, Y. Gao, T. Sun, Q. Yan, Y. Yang, *Appl. Catal. A* **380** (2010) 55–65.
- [34] M. Jacquin, D.J. Jones, J. Roziere, S. Albertazzi, A. Vaccari, M. Lenarda, L. Storaro, R. Ganzerla, *Appl. Catal. A* **251** (2003) 131–141.
- [35] N.T. Whilton, B. Berton, L. Bronstein, H.-P. Hentze, M. Antonietti, *Adv. Mater. (Weinheim, Ger.)* **11** (1999) 1014–1018.
- [36] T. Harada, S. Ikeda, Y.H. Ng, T. Sakata, H. Mori, T. Torimoto, M. Matsumura, *Adv. Funct. Mater.* **18** (2008) 2190–2196.
- [37] W. Huang, J.N. Kuhn, C.-K. Tsung, Y. Zhang, S.E. Habas, P. Yang, G.A. Somorjai, *Nano Lett.* **8** (2008) 2027–2034.
- [38] J.P.M. Niederer, A.B.J. Arnold, W.F. Holderich, B. Spliethof, B. Tesche, M. Reetz, H. Bonnemann, *Top. Catal.* **18** (2002) 265–269.
- [39] G.J. Hutchings, *Chem. Commun. (Cambridge, U.K.)* (2008) 1148–1164.
- [40] X. Yang, D. Chen, S. Liao, H. Song, Y. Li, Z. Fu, Y. Su, *J. Catal.* **291** (2012) 36–43.
- [41] S. Huh, H.-T. Chen, J.W. Wiench, M. Pruski, V.S.Y. Lin, *J. Am. Chem. Soc.* **126** (2004) 1010–1011.
- [42] C.-H. Tsai, H.-T. Chen, S.M. Althaus, K. Mao, T. Kobayashi, M. Pruski, V.S.Y. Lin, *ACS Catal.* **1** (2011) 729–732.
- [43] B. Zhu, M. Lazar, B.G. Trewyn, R.J. Angelici, *J. Catal.* **260** (2008) 1–6.
- [44] A. Beck, A. Horvath, A. Szucs, Z. Schay, Z. Horvath, Z. Zsoldos, I. Dekany, L. Guczi, *Catal. Lett.* **65** (2000) 33–42.
- [45] S. Papp, A. Szucs, I. Dekany, *Appl. Clay Sci.* **19** (2001) 155–172.
- [46] S. Gao, H. Zhang, X. Wang, W. Mai, C. Peng, L. Ge, *Nanotechnology* **16** (2005) 1234–1237.
- [47] W. Yan, V. Petkov, S.M. Mahurin, S.H. Overbury, S. Dai, *Catal. Commun.* **6** (2005) 404–408.
- [48] C. Marsden, E. Taarning, D. Hansen, L. Johansen, S.K. Klitgaard, K. Egeblad, C.H. Christensen, *Green Chem.* **10** (2008) 168–170.
- [49] E. Taarning, A.T. Madsen, J.M. Marchetti, K. Egeblad, C.H. Christensen, *Green Chem.* **10** (2008) 408–414.
- [50] K. Kaizuka, H. Miyamura, S. Kobayashi, *J. Am. Chem. Soc.* **132** (2010) 15096–15098.
- [51] W.J. Cui, Q. Xiao, S. Sarina, W.L. Ao, M.X. Xie, H.Y. Zhu, Z. Bao, *Catal. Today* **235** (2014) 152–159.
- [52] W.P. Deng, J.S. Chen, J.C. Kang, Q.H. Zhang, Y. Wang, *Chem. Commun. (Cambridge, U.K.)* **52** (2016) 6805–6808.
- [53] F. Gao, D.W. Goodman, *Chem. Soc. Rev.* **41** (2012) 8009–8020.
- [54] M.M. Schubert, S. Hackenberg, A.C. van Veen, M. Mueller, V. Plzak, R.J. Behm, *J. Catal.* **197** (2001) 113–122.
- [55] M. Haruta, M. Date, *Appl. Catal. A* **222** (2001) 427–437.
- [56] A. Wolf, F. Schueth, *Appl. Catal. A* **226** (2002) 1–13.
- [57] M.S. Chen, D.W. Goodman, *Catal. Today* **111** (2006) 22–33.
- [58] D.D. Das, A. Sayari, *J. Catal.* **246** (2007) 60–65.
- [59] A. Fihri, M. Bouhrara, B. Nekoueishahraki, J.-M. Basset, V. Polshettiwar, *Chem. Soc. Rev.* **40** (2011) 5181–5203.
- [60] J. Mondal, A. Modak, A. Bhaumik, *J. Mol. Catal. A Chem.* **350** (2011) 40–48.
- [61] N. Dimitratos, J.A. Lopez-Sanchez, D. Morgan, A.F. Carley, R. Tiruvalam, C.J. Kiely, D. Bethell, G.J. Hutchings, *Phys. Chem. Chem. Phys.* **11** (2009) 5142–5153.
- [62] I.W. Davies, L. Matty, D.L. Hughes, P.J. Reider, *J. Am. Chem. Soc.* **123** (2001) 10139–10140.